

Pseudospin Symmetry and Microscopic Origin of Shape Coexistence in the ^{78}Ni Region: A Hint from Lifetime Measurements

C. Delafosse,¹ D. Verney,^{1*} P. Marević,^{1,2} A. Gottardo,¹ C. Michelagnoli,³ A. Lemasson,³ A. Goasduff,⁴ J. Ljungvall,⁵ E. Clément,³ A. Korichi,⁵ G. De Angelis,⁴ C. Andreouiu,⁶ M. Babo,^{3,1} A. Boso,⁷ F. Didierjean,⁸ J. Dudouet,⁹ S. Franchoo,¹ A. Gadea,¹⁰ G. Georgiev,⁵ F. Ibrahim,¹ B. Jacquot,³ T. Konstantinopoulos,⁵ S. M. Lenzi,⁷ G. Maquart,⁹ I. Matea,¹ D. Mengoni,⁷ D. R. Napoli,⁴ T. Nikšić,¹¹ L. Olivier,¹ R. M. Pérez-Vidal,¹⁰ C. Portail,¹ F. Recchia,⁷ N. Redon,⁹ M. Siciliano,⁴ I. Stefan,¹ O. Stezowski,⁹ D. Vretenar,¹¹ M. Zielinska,¹² D. Barrientos,¹³ G. Benzoni,¹⁴ B. Birkenbach,¹⁵ A. J. Boston,¹⁶ H. C. Boston,¹⁶ B. Cederwall,¹⁷ L. Charles,⁸ M. Ciemala,¹⁸ J. Collado,¹⁹ D. M. Cullen,²⁰ P. Désesquelles,⁵ G. de France,³ C. Domingo-Pardo,¹⁰ J. Eberth,¹⁵ V. González,¹⁹ L. J. Harkness-Brennan,¹⁶ H. Hess,¹⁵ D. S. Judson,¹⁶ A. Jungclaus,²¹ W. Korten,¹² A. Lefevre,³ F. Legruel,³ R. Menegazzo,⁷ B. Million,¹⁴ J. Nyberg,²² B. Quintana,²³ D. Ralet,⁵ P. Reiter,¹⁵ F. Saillant,³ E. Sanchis,¹⁹ Ch. Theisen,¹² and J. J. Valiente Dobon⁴

¹*Institut de Physique Nucléaire, CNRS-IN2P3, Université Paris-Sud, Université Paris-Saclay, F-91406 Orsay, France*

²*CEA, DAM, DIF, F-91297 Arpajon, France*

³*Grand Accélérateur National d'Ions Lourds (GANIL), CEA/DSM-CNRS/IN2P3, Caen F-14076, France*

⁴*Istituto Nazionale di Fisica Nucleare, Laboratori Nazionali di Legnaro, I-35020 Legnaro, Italy*

⁵*CSNSM, CNRS-IN2P3, Université Paris-Sud, Université Paris-Saclay, F-91406 Orsay, France*

⁶*Department of Chemistry, Simon Fraser University, Burnaby, British Columbia, V5A 516, Canada*

⁷*Departmento di Fisica e Astronomia, Università di Padova, and INFN, Sezione di Padova, I-35131 Padova, Italy*

⁸*Université de Strasbourg, CNRS, IPHC UMR 7178, F-67000 Strasbourg, France*

⁹*Université Lyon, Université Lyon 1, CNRS/IN2P3, IPN-Lyon, F-69622, Villeurbanne, France*

¹⁰*IFIC, CSIC-Universitat Valencia, Apartado Oficial 22085, 46071 Valencia, Spain*

¹¹*Department of Physics, Faculty of Science, University of Zagreb, Bijenička c. 32, 10000 Zagreb, Croatia*

¹²*CEA de Saclay, IRFU, F-91191 Gif-sur-Yvette, France*

¹³*CERN, CH-1211 Geneva 23, Switzerland*

¹⁴*INFN Sezione di Milano, I-20133 Milano, Italy*

¹⁵*Institut für Kernphysik, Universität zu Köln, Zùlpicher Strasse 77, D-50937 Köln, Germany*

¹⁶*Oliver Lodge Laboratory, The University of Liverpool, Liverpool, L69 7ZE, United Kingdom*

¹⁷*Department of Physics, Royal Institute of Technology, SE-10691 Stockholm, Sweden*

¹⁸*The Henryk Niewodniczański Institute of Nuclear Physics, Polish Academy of Sciences, ul. Radzikowskiego 152, 31-342 Kraków, Poland*

¹⁹*Departamento de Ingeniería Electrónica, Universitat de Valencia, Burjassot, Valencia 46100, Spain*

²⁰*Nuclear Physics Group, Schuster Laboratory, University of Manchester, Manchester, M13 9PL, United Kingdom*

²¹*Instituto de Estructura de la Materia, CSIC, Madrid, E-28006 Madrid, Spain*

²²*Department of Physics and Astronomy, Uppsala University, SE-75120 Uppsala, Sweden*

²³*Laboratorio de Radiaciones Ionizantes, Universidad de Salamanca, E-37008 Salamanca, Spain*



(Received 18 May 2018; revised manuscript received 27 August 2018; published 9 November 2018)

Lifetime measurements of excited states of the light $N = 52$ isotones ^{88}Kr , ^{86}Se , and ^{84}Ge have been performed, using the recoil distance Doppler shift method and VAMOS and AGATA spectrometers for particle identification and gamma spectroscopy, respectively. The reduced electric quadrupole transition probabilities $B(E2; 2^+ \rightarrow 0^+)$ and $B(E2; 4^+ \rightarrow 2^+)$ were obtained for the first time for the hard-to-reach ^{84}Ge . While the $B(E2; 2^+ \rightarrow 0^+)$ values of ^{88}Kr , ^{86}Se saturate the maximum quadrupole collectivity offered by the natural valence ($3s$, $2d$, $1g_{7/2}$, $1h_{11/2}$) space of an inert ^{78}Ni core, the value obtained for ^{84}Ge largely exceeds it, suggesting that shape coexistence phenomena, previously reported at $N \lesssim 49$, extend beyond $N = 50$. The onset of collectivity at $Z = 32$ is understood as due to a pseudo-SU(3) organization of the proton single-particle sequence reflecting a clear manifestation of pseudospin symmetry. It is realized that

the latter provides actually reliable guidance for understanding the observed proton and neutron single particle structure in the whole medium-mass region, from Ni to Sn, pointing towards the important role of the isovector-vector ρ field in shell-structure evolution.

DOI: 10.1103/PhysRevLett.121.192502

Spin-orbit (SO) coupling and related effects are universal features of bound fermion systems, whether they are formed by electrons, quarks, nucleons, or hyperons. Ebran *et al.* [1] recently pointed out that the atomic nucleus occupies a particular position in this quantum landscape. Using the nonrelativistic reduction of the single-particle (SP) Dirac equation, they established a universal relationship between $|V_{LS}|/\hbar\omega_0$ (the amplitude of the SO splitting relative to the major harmonic oscillator shell gap) and $\eta = m/\Delta$ (the ratio between the mass of the particle and $\Delta = V - S$, the difference between vector and scalar potentials). Because in atomic nuclei $\eta \approx 1$, SO splitting is of the same order as the energy separation of the major shells and nuclear systems naturally stand at the edge of a predicted “giant” SO region [1]. While the coincidence $m \approx \Delta$ could seem to be just a natural curiosity, some more fundamental foundation in terms of quantum-chromodynamics (QCD) is suggested by in-medium QCD sum rules [2]. Nucleons experience two almost equivalently large potentials, the short-range repulsive vector potential $V \approx 350$ MeV and medium-range attractive scalar potential $S \approx -400$ MeV, leading to $\Delta \approx 750$ MeV of the order of magnitude of the nucleon mass ($m \approx 940$ MeV) itself, explaining $\eta \approx 1$ and the large nuclear SO coupling. The counterpart of this QCD-emerging quasiequality $S \approx -V$ is that the net binding potential $\Sigma = V + S$ is inherently small, leading to the far-reaching consequence that pseudospin symmetry (PSS) is approximately realized in nuclei [3–5]. Manifestations of this symmetry were early noted [6,7] in the empirical spherical SP-energy sequences where, especially for heavy nuclei, one observed quasidegeneracy of doublets characterized by the sets of quantum numbers $(n, \ell, j = \ell + 1/2)$ and $(n - 1, \ell + 2, j = \ell + 3/2)$. This suggested a fruitful relabeling to pseudoradial, pseudo-orbital, and pseudospin quantum numbers ($\tilde{n} = n - 1, \tilde{\ell} = \ell + 1, \tilde{s} = s$) thus associating these doublets to pseudospin-orbit (PSO) $j = \tilde{l} \pm \tilde{s}$ partners (PSOPs) whose splittings could be related to the depth or radial derivative of the Σ potential [3,8]. Spectroscopic manifestations of PSS are far from being restricted to spherical SP degeneracy, since PSS has as a direct consequence (and provides the microscopic foundation for) the realization of a variant of Elliott’s SU(3) symmetry called the pseudo-SU(3) symmetry for many-nucleon wave functions. PSS has been indeed recognized as the underlying mechanism leading to a wealth of salient spectroscopic features in the phenomenology of superdeformed nuclei (identical bands for instance [9,10]). However, the full expression

and consequences of this symmetry on the structure of exotic nuclei having unusual neutron-to-proton ratios remain largely unexplored.

The present experimental investigation was prompted by the recent, until then unexpected, discovery of evidence for shape coexistence in the ^{78}Ni region [11,12]. It will be shown that PSS not only provides a natural explanation for the occurrence of shape coexistence around $Z \approx 32, N \approx 50$ but also reliable guidance to understand the observed proton and neutron SP structure in the whole medium-mass region, from Ni to Sn, pointing towards the important role of the isovector-vector ρ field [13] in shell evolution.

Gottardo *et al.* [11] discovered that the first excited state of the $N = 48$ even-even nucleus ^{80}Ge is actually a $J^\pi = 0^+$ state, lying slightly below the normal one-phonon 2^+ state in the excitation spectrum. They interpreted this state as originating from a configuration involving neutron-pair promotions across the $N = 50$ gap and collecting sufficient proton-neutron quadrupole correlations to counterbalance a SP-promotion cost, apparently also reduced thanks to favorable monopole drifts. The primary objective of the present work was to investigate further this scenario by studying the origin of collective quadrupole effects beyond the $N = 50$ shell gap, focusing on their evolutions in $N = 52$ even-even isotones approaching $Z = 28$ thanks to the measurement of reduced electric quadrupole transition probabilities $B(E2; 2^+ \rightarrow 0^+)$. This was an *a priori* demanding task in view of the accumulation of evidence—though so far only model-dependently inferred—for triaxiality approaching $Z = 32$ [14,15]. The measurement of 2^+ state lifetimes seemed then the ideal approach, because the extraction of $B(E2)$ from Coulomb-excitation cross sections might be distorted either by unmeasured diagonal $E2$ matrix elements having unexpected values originating from triaxial dynamics or, more importantly, by transitions to yet unobserved or unidentified low-lying 0^+ states originating from shape coexistence.

The experiment was performed at GANIL. The $N = 52$ ^{88}Kr , ^{86}Se , and ^{84}Ge nuclei were produced by fusion and transfer fission (with a cross-section ratio 8/2 for the two processes [16]) of a ^{238}U beam at 6.2 AMeV on a Be target with a thickness of 2.07 mg/cm². The average intensity of the beam was 0.25 pA. The fission fragments were identified and their velocities were determined with the magnetic spectrometer VAMOS++ [17], placed at 28° with respect to the beam direction, using the procedure already described in Ref. [18]. A total of $\approx 1.5 \times 10^7$ fission-fragment events were identified out of which the ^{88}Kr ,

TABLE I. Lifetime results, associated $B(E2)$, and comparison with available data in literature. The value marked with (*) is an effective lifetime.

Nucleus	$J_i^\pi \rightarrow J_f^\pi$	E_γ [keV]	This work		Literature	
			τ [ps]	$B(E2; J_i^\pi \rightarrow J_f^\pi)$ [$e^2 \text{ fm}^4$]	τ [ps]	$B(E2; J_i^\pi \rightarrow J_f^\pi)$ [$e^2 \text{ fm}^4$]
^{88}Kr	$2^+ \rightarrow 0^+$	775.4(1)	$10.6^{+4.8}_{-5.0}$	$273.6^{+244.3}_{-85.3}$	16.0(17) [30]	262(38) [31]
^{86}Se	$2^+ \rightarrow 0^+$	704.0(1)	$10.3^{+1.2}_{-2.2}$	456^{+124}_{-48}	$10.8^{+6.9}_{-3.7-0.3}$ [25]	422(64) [31]
^{84}Ge	$2^+ \rightarrow 0^+$	624.3(9)	$13.8^{+7.9}_{-9.8}$	$621.2^{+1522.0}_{-226.2}$
	$4^+ \rightarrow 2^+$	805.4(11)	$10.3^{+3.0}_{-6.5}$ (*)	$232.9^{+398.4}_{-52.5}$

^{86}Se , and ^{84}Ge residues represented 3.0%, 1.7%, and 0.06%, respectively.

The prompt gamma rays were detected by the AGATA array [19,20]. The setup comprised eight triple cluster modules placed at 18.6 cm from the target. The gamma-emission spectrum of each nucleus of interest was Doppler corrected event by event using the velocity vector measured in VAMOS and the position of the first gamma interaction in AGATA with a full width half maximum resolution of about 5 mm [21]. The energies of gamma rays were obtained by applying off line the OFT gamma-ray tracking algorithm [22].

Lifetime measurements were performed using the well-established recoil distance Doppler shift (RDDS) technique [23]. A Mg degrader foil with a thickness of 5 mg/cm² was maintained downstream from the production target at three distances, $D = 120, 270,$ and $520 \mu\text{m}$, with a precision of 10 μm , for 75 h, 75 h, and 85 h, respectively, of measuring time by using the Orsay Universal Plunger System (OUPS) [24]. Depending on the lifetime τ of the state of interest and the distance D , gamma rays were emitted partially before and after the degrader at respective fission-product recoil velocities β_{before} and β_{after} . Photopeaks appeared then in the spectra as doublets of Doppler unshifted and shifted components, with intensities I_U and I_S , respectively. The former corresponds to gamma emission after the degrader corrected for β_{after} precisely determined from VAMOS information [$\beta_{\text{after}} = 0.096(11)$], the latter to gamma emission before the degrader, at velocity $\beta_{\text{before}} > \beta_{\text{after}}$, slightly shifted towards lower energies (because AGATA was located at backward angles).

The quantities of interest were ratios $R(t_D) = \{[I_U(t_D)]/[I_S(t_D) + I_U(t_D)]\}$ associated to flight time t_D at each D . Variants of the RDDS technique suitable for low-statistics, low D -number cases developed in Refs. [25,26] were adopted for the present analysis. Seven, five, and two transitions in ^{88}Kr , ^{86}Se , and ^{84}Ge , already identified in Refs. [15,27,28], respectively, could be studied and the effective or intrinsic lifetimes (uncorrected or corrected for the feeding lifetimes, respectively) of the corresponding decaying states were extracted. We report in Table I results relevant for the present discussion. Further analysis details and lifetime results [29] will be given elsewhere. As can be

seen in this table, our lifetime and associated $B(E2)$ results are in excellent agreement with previous RDDS and Coulomb excitation measurements for ^{88}Kr and ^{86}Se . $B(E2; 4^+ \rightarrow 2^+)$ and $B(E2; 2^+ \rightarrow 0^+)$ values were obtained for the first time for the hard-to-reach ^{84}Ge isotope. This result deserves then a few more detailed comments. Because of low statistics, the RDDS-analysis variant developed in Ref. [25] had to be preferred, which consists in summing the statistics obtained over all distances and determining the lifetime as illustrated in Fig. 1. After this summation process, a (so-called cumulative) ratio $R(\tau)$ forming a continuous function of the lifetime τ can be obtained from the relevant set of Bateman equations, including the relative statistics weight at each distance, that intercepts a horizontal line representing the measured cumulative R_{exp} . The central lifetime value stems directly from the projection of the interception point on the τ axis. Following the method of Ref. [25], the complex error propagations were treated by 10⁶ Monte Carlo random draws in Gaussian envelopes around the central $R(\tau)$ curve and R_{exp} line. Clearly, this procedure leads to inherently asymmetric error bars. In the present case, as no feeding to the 4^+ state was observed, τ_{4^+} is an effective lifetime, i.e., an *upper* intrinsic lifetime [providing a *lower* $B(E2; 4^+ \rightarrow 2^+)$] estimate. On the contrary, τ_{2^+} is an intrinsic lifetime, cleared of the time contribution from the apparent lifetime of the

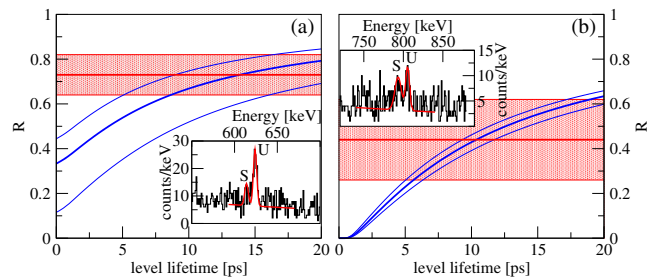


FIG. 1. Graphical determination of the lifetimes of the 2^+ (a) and 4^+ (b) excited states of ^{84}Ge (see text). The shaded area and the two thinner curves materialize the 1σ uncertainty regions. The insets show the relevant regions of the gamma spectrum, with the shifted and unshifted photo-peak components marked with “S” and “U,” respectively.

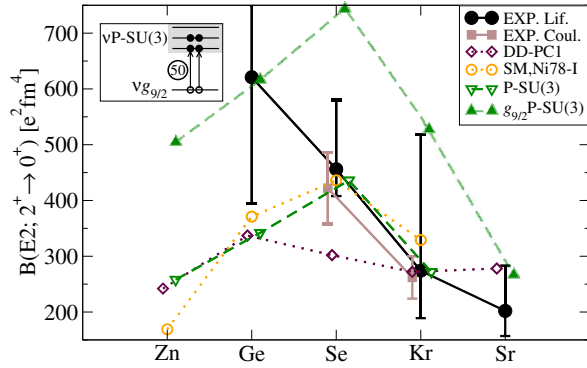


FIG. 2. $B(E2; 2^+ \rightarrow 0^+)$ systematics of the light $N = 52$ even-even isotones from $Z = 38$ down to $Z = 30$. “EXP. Lif.”: experimental values from lifetimes measurements (this work, except Sr [34]); “EXP. Coul.”: experimental values from Coulomb excitation measurements [31]; “DD-PC1”: beyond mean-field calculations using the relativistic functional DD-PC1 (this work); “SM, Ni78-I”: shell-model calculations from [32]; “ $(g_{9/2})$ P-SU(3)”: pseudo-SU(3) limit [32] (or including one $N = 50$ core-breaking $g_{9/2}$ pair promotion, as illustrated by the inset).

$4^+ \rightarrow 2^+$ feeding transition. The observed relative intensities of the $4^+ \rightarrow 2^+$ and $2^+ \rightarrow 0^+$ transitions suggested 10(10)% unobserved feeding to the 2^+ state which was assumed to come from a direct feeding by the reaction. The effect of neglecting the contribution from a hypothetical long-lived unobserved gamma feeding is to *overestimate* τ_{2^+} , i.e., to *underestimate* the corresponding $B(E2; 2^+ \rightarrow 0^+)$ probability.

The obtained $B(E2)$ values are placed in the systematics of light $N = 52$ isotones in Fig. 2, where comparison with several calculations is also provided. Shell-model results from Ref. [32] (open circles), assuming an inert ^{78}Ni core, are in excellent agreement with the experimental central values (closed circles) obtained for ^{88}Kr and ^{86}Se . Interestingly enough, both shell-model and experimental values exhaust the limit for pure pseudo-SU(3) symmetry (down triangles) for these two isotones. This limit was obtained [32] by assuming that the $(Z - 28)$ protons lie in a $\tilde{s}\tilde{d}$ block formed by the $f_{5/2}p$ orbits and the two neutrons in a $\tilde{p}\tilde{f}$ block formed by the $g_{7/2}ds$ orbits. This clearly means that the quadrupole coherence offered by this subspace is maximally expressed in these two nuclei. In contrast, both shell-model and pseudo-SU(3) values barely reach the lower tip of the experimental error bar for ^{84}Ge . Statistically speaking, this means that there is around 85% chance that the actual $B(E2)$ value lies higher, i.e., that a fraction—possibly large—of the quadrupole correlations expressed in ^{84}Ge lies outside the limits of the valence of an inert ^{78}Ni core. For instance, considering the promotion of a $g_{9/2}$ neutron pair across the $N = 50$ gap to the $\tilde{p}\tilde{f}$ block (up triangles in Fig. 2) one obtains $B(E2; 2^+ \rightarrow 0^+) = 616 e^2 \text{fm}^4$, a value strikingly close to the experimental one. Following Ref. [33], one can also understand the situation as originating from 12

neutrons filling the SP sequence ($g_{9/2}, d_{5/2}, s_{1/2}$) considered as forming a quasi-SU(3) subspace. In that case, a similarly close value of $600 e^2 \text{fm}^4$ is obtained. We note that such an interpretation would imply that inversion of normal and intruder configurations has already occurred in ^{84}Ge while it seems yet not to be the case in ^{80}Ge [11]. Because of the large uncertainty, the obtained $B(E2)$ cannot be used to determine unambiguously the exact component along the ^{78}Ni core-breaking neutron (np-nh) configuration of the ^{84}Ge ground state. Nevertheless, we will try with the following discussion to fully explore the physical consequences of the assumption that the obtained central value is the correct one.

The trend drawn by the central values in Fig. 2 is indeed clear and it is the one of a shape transition from $Z = 34$ to 32 at $N = 52$. One must then investigate the following question: What is the microscopic origin of such an onset of quadrupole coherence specifically at $Z = 32$? A fully microscopic approach, free from valence space limitations, should show the way to an explanation. A self-consistent mean field calculation using a relativistic functional was chosen in order to highlight the possible PSS roots of this phenomenon. Following Refs. [35,36], constrained mean-field (CMF) calculations of energy surfaces as functions of quadrupole (β, γ) deformation parameters were performed using the relativistic functional DD-PC1 [37]. The collective Hamiltonian was subsequently diagonalized to obtain the spectroscopy of the $30 \leq A \leq 38$ $N = 52$ even-even isotones. The resulting $B(E2)$ values are reported in Fig. 2 (open diamonds). The obtained trend from $Z = 36$ to 32 is an almost ideal linear increase as indeed observed experimentally (it is the only calculation in Fig. 2 showing this feature). The slope, however, is lower than the experimental one. This is expected: it is well known that the description of the quadrupole properties from beyond mean-field treatments deteriorates (for other functionals as well, see e.g., [38]) while approaching shell closures. From $Z = 36$ to 32 one gets closer to both $Z = 28$ and $N = 50$ magic numbers and this effect is further enhanced. Nevertheless, because the trend is correct, the obtained proton mean-field SP sequence can now be used to explain an increased quadrupole collectivity in ^{84}Ge . As can be seen in the inset of Fig. 3, the K -orbital sequence stemming from the $1f_{5/2}2p$ (or $\tilde{s}\tilde{d}$) system actually forms a textbook example of an emerging sequence of deformed pseudospin $[\tilde{N}n_3\tilde{\Lambda}K = \tilde{\Lambda} \pm 1/2]$ doublets as described in Ref. [39]. In the central panel, the Fermi level (dashed-dotted line) crosses a pronounced triaxial gap maximally opened at maximum triaxiality, $\gamma \approx 30^\circ$. Starting from the prolate side, for $(\beta = 0.2, \gamma \gtrsim 0^\circ)$, where the memory of the intrinsic-axis projection number K is not completely lost, one observes an apparent repulsion of the $[\tilde{2}11 K = 1/2, 3/2]$ components of $\tilde{s}\tilde{d}$ parentage, as if due to strong $\Delta K = \pm 1$ Coriolis mixing (thus opening the gap) in a way reminiscent of the famous mixing of pseudospin aligned

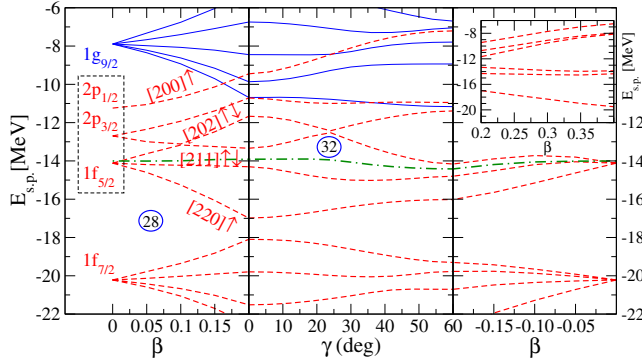


FIG. 3. Relativistic-CMF proton SP energy in canonical basis for ^{84}Ge . Solid (blue), dashed (red), and dashed-dotted (green) curves correspond to positive parity, negative parity, and Fermi levels, respectively. Left and right panels show the evolution of the SP levels with β at axial $\gamma = 0^\circ$ and $\gamma = 60^\circ$ limits, respectively, while the central one shows evolution with the asymmetry gamma parameter at fixed mean-field minimum ($\beta = 0.2$). The pseudo-Nilsson labels $[\tilde{N}n_3\tilde{\lambda}]$ of the deformed states stemming from the $\tilde{s}\tilde{d}$ spherical system (dotted frame) are reported close to the relevant levels. Their evolution towards pseudospin partners degeneracy at larger deformation is shown in the inset.

and unaligned bands based on neutron $K = 1/2, 3/2$ Nilsson orbits of $2\tilde{d}$ origin in $^{187,189}\text{Os}$ [40].

Therefore, it becomes clear that it is this specific $\pi 1f_{5/2}2p$ SP arrangement that triggers quadrupole coherence in ^{84}Ge —and it finds its roots in PSS as we will now demonstrate. The evolution with isospin of this $1f_{5/2}2p$ system is most clearly manifested in the structure of the neutron-rich Cu isotopes and its experimental investigation has been pursued for exactly two decades (see Ref. [41] and references therein). The faster increase of the $1f_{5/2}$ binding compared to the one of $2p_{3/2}$, with increasing neutron number, has generally been ascribed to Ostuka’s tensor mechanism [42]. However, the necessary counterpart is a loss of $1f_{7/2}$ binding energy and the closing of the $Z = 28$ gap (Fig. 4 in Ref. [42]) which should have led to the observation of increasingly large $1f_{7/2}$ strength in the low lying $7/2^-$ Cu excited states approaching $N = 50$. This is at odds with any of the recent experimental findings [41,43]. PSS, on the contrary, explains nicely this feature because $1f_{7/2}$ is a “pseudospin-unpaired state” [4] (it has no PSOP) while $1f_{5/2}2p_{3/2}$ are PSOPs. The empirical proton $1\tilde{d}$ reduced PSO splitting Δ_{PSO} is reported as a function of isospin T in Fig. 4, and compared to the well known [4] proton $2\tilde{p}$ and $1\tilde{f}$ doublets of the Sb ($Z = 51$) chain: the behavior is strikingly similar. The loss of PSS (increase of Δ_{PSO}) while approaching the $N = 50$ shell closure ($T = 21/2$) is probably related to the nodal structure of the proton and neutron SP states involved, as a comparison with the Ce case (approaching $N = 126$) [44] would suggest.

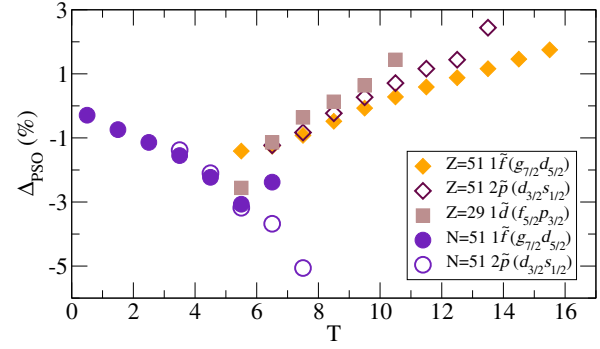


FIG. 4. Reduced PSO splitting $\Delta_{\text{PSO}} = (\epsilon_{j_+} - \epsilon_{j_-}) / [\hbar\omega(2\tilde{l} + 1)]$ as a function of isospin T for the $2\tilde{p}$ and $1\tilde{f}$ doublets in Sb isotopes and $N = 51$ isotones and for the $1\tilde{d}$ doublet in Cu isotopes extracted from spectroscopic data [34,41].

Concerning now the origin of the *neutron* SP structure of ^{84}Ge , the $2\tilde{p}$ and $1\tilde{f}$ doublets are actually also recognizable in the spectroscopy of the heaviest $N = 51$ isotones, and their Δ_{PSO} are represented in Fig. 4. The evolution with T is the opposite of the one for protons, this is a well-known result of relativistic mean field and originates from the ρ -meson interaction which is repulsive for neutrons and attractive for protons (see Refs. [4,5] and references therein, in particular Ref. [45]). As discussed in the introduction, PSS is restored (Δ_{PSO} is reduced) for vanishing binding Σ potential. But, following the conclusions of Ref. [45], decrease and increase of the nuclear radius and diffusivity, respectively, both lead to a reduction of Δ_{PSO} which can become inverted for sufficiently weak Σ . For the $N = 51$ $2\tilde{p}$ and $1\tilde{f}$ doublets, starting from a neutron pseudospin symmetric ^{101}Sn (see Fig. 4) and increasing T (decreasing mass number), all effects contribute jointly to increase an inverted Δ_{PSO} . This not only elegantly explains the otherwise puzzling observation of the $3s_{1/2}$ ($2\tilde{p}$ doublet member) lowering [46], but also implies a $2d_{5/2}$ ($1\tilde{f}$ doublet member) lowering towards ^{78}Ni . The latter orbit, by getting closer to the pseudospin-unpaired state $1g_{9/2}$, reduces the $N = 50$ gap: precisely the second ingredient needed [11] to explain the emergence of shape coexistence phenomena in the ^{78}Ni region and its realization in ^{84}Ge . The Δ_{PSO} slope breaks and increases around $T = 4$ (Fig. 4), further suggesting an increased neutron diffusivity towards ^{78}Ni . This may well happen due to the formation of a neutron skin, actually predicted by relativistic Hartree-Fock-Bogoliubov (HFB) calculations [44], whose spectroscopic manifestations have just been experimentally noticed [47].

In conclusion, thanks to the superior resolving power of AGATA and precise gamma-emission angle determination offered by the advent of gamma tracking, the RDDS lifetime measurement of excited states in light $N = 52$ isotones could be extended down to the exotic ^{84}Ge . Our data suggest for the first time a shape transition from

$Z = 34$ (soft triaxial) to $Z = 32$ (prolate deformed), a result all the more unexpected as the shell model predicts a “fifth island of inversion” only for much lighter ($Z < 28$) systems [48]. Isospin asymmetry of the PSS is the hidden architect of the proton and neutron SP organization, preparing the fertile ground for its occurrence. It is a manifestation of the tensor ρ -exchange potential, but as PSS is a dynamical symmetry in nature, originating from the cancellation of several terms contributing to the SP energy [49], it contains richer spin-isospin properties than can be exhaustively captured in the usual tensor schematic picture. In particular, since this short-range potential is essentially manifested through exchange terms it naturally links shell evolution and formation of giant halos or neutron skins [44] involving large s and p orbits—whose spectroscopic expression has incidentally long passed unnoticed in the ^{78}Ni region [47]. Thus, while quantitative relativistic calculations and more precise experimental results for this mass sector are certainly called for, it can already be conjectured that PSS concepts and the related role of the ρ potential are to become more and more useful for understanding observed shell evolutions in very neutron-rich, medium-to-heavy mass nuclei.

D. Ve. expresses his gratitude to K. Sieja for fruitful discussions, to J.-P. Ebran and E. Khan for their interest in this work and careful reading of the Letter and to F. Farget for decisive help with a judicious choice of the VAMOS angle. We acknowledge the important technical contributions of J. Goupil, G. Fremont, L. Ménager, J. Ropert, C. Spitaels, and the GANIL accelerator staff. The authors acknowledge support from the European Union Seventh Framework Programme through ENSAR, Contract No. 262010. The work of T. N. and D. Vr. was supported by the QuantiXLie Centre of Excellence (Grant No. KK.01.1.1.01.0004) co-financed by the European Regional Development Fund and the Cohesion Fund from Ministry of Science and Technology of Croatia within the Operational Program “Competitiveness and Cohesion”. The work of M. C. was supported by the Polish National Science Centre (NCN), Contract No. 2016/22/M/ST2/00269. C. A. also acknowledges the support from the Natural Sciences and Engineering Research Council of Canada.

*Corresponding author
 verney@ipno.in2p3.fr

- [1] J.-P. Ebran, E. Khan, A. Mutschler, and D. Vretenar, *J. Phys. G* **43**, 085101 (2016).
- [2] T. D. Cohen, R. J. Furnstahl, and D. K. Griegel, *Phys. Rev. Lett.* **67**, 961 (1991).
- [3] J. N. Ginocchio, *Phys. Rev. Lett.* **78**, 436 (1997).
- [4] J. N. Ginocchio, *Phys. Rep.* **414**, 165 (2005).
- [5] H. Liang, J. Meng, and S.-G. Zhou, *Phys. Rep.* **570**, 1 (2015).
- [6] K. Hecht and A. Adler, *Nucl. Phys.* **A137**, 129 (1969).
- [7] A. Arima, M. Harvey, and K. Shimizu, *Phys. Lett.* **30B**, 517 (1969).
- [8] J. Meng, K. Sugawara-Tanabe, S. Yamaji, P. Ring, and A. Arima, *Phys. Rev. C* **58**, R628 (1998).
- [9] W. Nazarewicz, P. J. Twin, P. Fallon, and J. D. Garrett, *Phys. Rev. Lett.* **64**, 1654 (1990).
- [10] F. S. Stephens *et al.*, *Phys. Rev. Lett.* **65**, 301 (1990).
- [11] A. Gottardo *et al.*, *Phys. Rev. Lett.* **116**, 182501 (2016).
- [12] X. F. Yang *et al.*, *Phys. Rev. Lett.* **116**, 182502 (2016).
- [13] K. Erkelenz, *Phys. Rep.* **13**, 191 (1974).
- [14] M. Lebois *et al.*, *Phys. Rev. C* **80**, 044308 (2009).
- [15] M. Lettmann *et al.*, *Phys. Rev. C* **96**, 011301 (2017).
- [16] A. Navin *et al.*, *Phys. Lett. B* **728**, 136 (2014).
- [17] M. Rejmund *et al.*, *Nucl. Instrum. Methods A* **646**, 184 (2011).
- [18] J. Dudouet *et al.*, *Phys. Rev. Lett.* **118**, 162501 (2017).
- [19] S. Akkoyun *et al.*, *Nucl. Instrum. Methods A* **668**, 26 (2012).
- [20] E. Clément *et al.*, *Nucl. Instrum. Methods A* **855**, 1 (2017).
- [21] B. Bruyneel, B. Birkenbach, and P. Reiter, *Eur. Phys. J. A* **52**, 70 (2016).
- [22] A. Lopez-Martens, K. Hauschild, A. Korichi, J. Roccoz, and J.-P. Thibaud, *Nucl. Instrum. Methods A* **533**, 454 (2004).
- [23] A. Dewald, O. Moller, and P. Petkov, *Prog. Part. Nucl. Phys.* **67**, 786 (2012).
- [24] J. Ljungvall *et al.*, *Nucl. Instrum. Methods A* **679**, 61 (2012).
- [25] J. Litzinger *et al.*, *Phys. Rev. C* **92**, 064322 (2015).
- [26] F. Didierjean *et al.*, *Phys. Rev. C* **96**, 044320 (2017).
- [27] A. Astier *et al.*, *Phys. Rev. C* **88**, 024321 (2013).
- [28] F. Drouet *et al.*, *EPJ Web Conf.* **62**, 01005 (2013).
- [29] C. Delafosse, Etude des dérivées monopolaires neutron au-delà de ^{78}Ni par spectroscopie γ avec BEDO à ALTO et AGATA au GANIL, Ph.D. thesis, Université Paris Saclay, 2018, <http://www.theses.fr/s144799>.
- [30] D. Mücher *et al.*, *AIP Conf. Proc.* **1090**, 587 (2009).
- [31] B. Elman *et al.*, *Phys. Rev. C* **96**, 044332 (2017).
- [32] K. Sieja, T. R. Rodríguez, K. Kolos, and D. Verney, *Phys. Rev. C* **88**, 034327 (2013).
- [33] A. P. Zuker, A. Poves, F. Nowacki, and S. M. Lenzi, *Phys. Rev. C* **92**, 024320 (2015).
- [34] <http://www.nndc.bnl.gov>.
- [35] T. Nikšić, Z. P. Li, D. Vretenar, L. Próchniak, J. Meng, and P. Ring, *Phys. Rev. C* **79**, 034303 (2009).
- [36] T. Nikšić, P. Marević, and D. Vretenar, *Phys. Rev. C* **89**, 044325 (2014).
- [37] T. Nikšić, D. Vretenar, and P. Ring, *Phys. Rev. C* **78**, 034318 (2008).
- [38] J. P. Delaroche, M. Girod, J. Libert, H. Goutte, S. Hilaire, S. Péru, N. Pillet, and G. F. Bertsch, *Phys. Rev. C* **81**, 014303 (2010).
- [39] A. Bohr, I. Hamamoto, and B. R. Mottelson, *Phys. Scr.* **26**, 267 (1982).
- [40] A. M. Bruce, C. Thwaites, W. Gelletly, D. D. Warner, S. Albers, M. Eschenauer, M. Schimmer, and P. vonBrentano, *Phys. Rev. C* **56**, 1438 (1997).
- [41] L. Olivier *et al.*, *Phys. Rev. Lett.* **119**, 192501 (2017).
- [42] T. Otsuka, T. Suzuki, R. Fujimoto, H. Grawe, and Y. Akaishi, *Phys. Rev. Lett.* **95**, 232502 (2005).
- [43] P. Morfouace *et al.*, *Phys. Lett. B* **751**, 306 (2015).

- [44] W.H. Long, P. Ring, J. Meng, N. Van Giai, and C. A. Bertulani, *Phys. Rev. C* **81**, 031302 (2010).
- [45] P. Alberto, M. Fiolhais, M. Malheiro, A. Delfino, and M. Chiapparini, *Phys. Rev. Lett.* **86**, 5015 (2001).
- [46] J. S. Thomas *et al.*, *Phys. Rev. C* **76**, 044302 (2007).
- [47] A. Gottardo *et al.*, *Phys. Lett. B* **772**, 359 (2017).
- [48] F. Nowacki, A. Poves, E. Caurier, and B. Bounthong, *Phys. Rev. Lett.* **117**, 272501 (2016).
- [49] P. Alberto, M. Fiolhais, M. Malheiro, A. Delfino, and M. Chiapparini, *Phys. Rev. C* **65**, 034307 (2002).